Volume 1 | Number 1 | Jan 2013 | Pages 1–100

Journal of
Materials Chemistry B

Materials for biology and medicine
www.rsc.org/materialsB

ROYAL SOCIETY
OF CHEMISTRY

ROYAL SOCIETY
OF CHEMISTRY

www.rsc.org/materialsB

Journal Name

ARTICLE

Development of green to near-infrared turn-on fluorescent probes for multicolour imaging of nitroxyl in living system†

Baoli Dong,[a] Kaibo Zheng,[b] Yonghe Tang,[a] and Weiying Lin *[a,b]

Nitroxyl (HNO) is one of important reactive nitrogen species (RNS) and has significant biological activities with numerous therapeutic potential. Herein, three novel turn-on probes (**NP-1~3**) based on the structurally related dyes with different emission colors as the fluorescent sacffolds, have been developed for detecting HNO in biological systems. The probes exhibit high sensitivity, excellent selectivity, desirable performance at physiological pH, and low cytotoxicity. By incubating the living cells with these probes simultaneously, we demonstrate the multicolor imaging of HNO with emission colors in the range of green to near-infrared (NIR) in the living systems for the first time. Furthermore, the probe **NP-3** responds to HNO with a significant turn-on NIR fluorescence signal upon excitation at the NIR region, and it is successfully applied for sensing HNO in the living mice.

Introduction

The reactive nitrogen species (RNS) are a class of chemically reactive nitrogen-containing species, and play important roles in a number of biological functions in mammalian system. For example, the endogenous generated nitric oxide (NO), one of typical RNS, could serve as a signaling molecule and exhibit beneficiary effects to many pathophysiological conditions, such as maintaining vascular tone, regulating central nervous system.[1] More recently, the one-electron reduced and protonated derivative of NO, nitroxyl (HNO), has been found to show numerous biological activities with significant therapeutic potential including utilization as anti-cancer drug, treatment of heart failure, and protection tissue against reperfusion injury. Furthermore, HNO also possesses distinguishable physiological and pharmacological properties from NO.[1-3] Therefore, it is of high interest to develop sensitive and selective methods for detecting HNO in biosystem.

Up to date, many traditional analytical methods for HNO detection including colorimetric methods,[4-5] EPR,[6] mass spectrometry[7] and electrochemical analysis[8] have been developed and could provide sensitive and precise analysis, but their requirements for the sophisticated instrumentation, the complicated sample preparation and the destruction of cells or tissues block their applications in living biological system. By contrast, the fluorescence analytical method with the help of fluorescent probes have been widely used for detecting bioactive molecules due to the low cost, simple operation procedure, high selectivity and sensitivity as well as real-time imaging.[9-25] Thus far, many fluorescent probes for HNO with excellent properties have been developed.[26-36] However, most of these probes utilize the changes in emission intensity as sensing signal, which generally tend to be interfered by the fluctuation in excitation light, inhomogeneous cellular distribution, or the environment around the probe such as pH, temperature, polarity. In comparison, the multicolor imaging, taking more than two emission bands as sensing signals, could furthest eliminate these disturbances to afford precise detection for HNO. Thus, the development of fluorescent probes for multicolor imaging of HNO in biological system has attracted great attention.

Utilizing the multiple fluorescent probes simultaneously in one of the same specimen as long as they have sufficiently minimized spectral overlap, the optical microscopy could provide multicolor fluorescent images to precisely detect biomolecules in living system.[37-40] It is possible even with a simple optical setup to clearly distinguish different wavelengths with the help of fluorescent probes. In other words, using different filter sets, it could image multicolor simultaneously with minimal crosstalk. Recently, Lippard's group reported the first application of a multicolour imaging experiment to study the cellular chemistry of HNO.[26] They demonstrated that the probe **CuDHX1** could be used to detect exogenous HNO in live mammalian cells, and may be employed for multicolor/bi-analyte microscopic imaging in conjunction with the zinc-specific fluorescent probe **ZP1**. However, the two probes (**CuDHX1** and **ZP1**) were used for multicolor imaging of two different analytes, HNO and zinc ions. To our best knowledge, the multicolor imaging of HNO in living system directly through two or

a. Institute of Fluorescent Probes for Biological Imaging, School of Chemistry and Chemical Engineering, School of Biological Science, University of Jinan, Jinan, Shandong 250022, P.R. China, E-mail: weiyinglin2013@163.com
b. State Key Laboratory of Chemo/Biosensing and ChemometricsCollege ofChemistry and Chemical Engineering, Hunan university, Changsha, Hunan 410082, P. R. China

more fluorescent probes with different emission wavelengths has not been reported yet.

Herein, we describe three novel, selective and sensitive turn-on fluorescent probes for detecting HNO, utilizing triphenylphosphine as response site. The probes could exhibit different emission colors from green to near-infrared (NIR) in response to HNO in aqueous solution and cells. By incubating the same cells with these probes, we firstly describe the multicolor imaging of HNO with emission colors in the range of green to near-infrared (NIR) in living system. In addition, the probe **NP-3**, could respond to HNO with obvious turn-on NIR fluorescence upon excitation at NIR region, and is successfully applied for sensing HNO in living mice.

Experimental

Materials and instruments

Unless otherwise stated, all reagents were purchased from commercial suppliers and used without further purification. Solvents were purified by standard methods prior to use. Twice-distilled water was used throughout all experiments. Low resolution mass spectra were performed using an LCQ Advantage ion trap mass spectrometer from Thermo Finnigan or Agilent 1100 HPLC/MSD spectrometer; High-resolution electronspray (EI-HRMS) mass spectra were obtained from Bruker APEX IV-FTMS 7.0T mass spectrometer. NMR spectra were recorded on an INOVA-400 spectrometer, using TMS as an internal standard; Electronic absorption spectra were obtained on a LabTech UV Power spectrometer. Photoluminescent spectra were recorded with a HITACHI F4600 fluorescence spectrophotometer. Data were expressed as mean ± standard deviation (SD) of three separate measurements. Cells imaging was performed with an Olympus fluorescence microscopy equipped with a cooled CCD camera or Nikon A1R confocal microscope. The pH measurements were carried out on a Mettler-Toledo Delta 320 pH meter. TLC analysis was performed on silica gel plates and column chromatography was conducted over silica gel (mesh 200-300), both of which were obtained from the Qingdao Ocean Chemicals.

Synthesis of probes NP-1~3

In a 25 mL round bottomed flask were added 2-(diphenylphosphino) benzoic acid (37 mg, 0.12 mmol), OH-containing fluorophore (0.10 mmol), DMAP (8.7 mg, 0.07 mmol), DCC (26.8 mg, 0.13 mmol), and anhydrous CH_2Cl_2 (3 mL). After stirred at room temperature for 8 hours under N_2 atmosphere, the reaction mixture was concentrated under vacuum, and then the crude product was purified by silica column chromatography to afford the desired products.

NP-1 was obtained as a yellow solid (40.8 mg, 0.07 mmol, 70%), ^{1}H NMR (400 MHz, CDCl$_3$) δ6.84 (d, J = 8.0 Hz, 1H), 7.00-7.03 (q, 1H), 7.28-7.36(m, 11H), 7.40-7.54 (m, 6H), 7.94(d, J = 8.0 Hz, 1H), 8.08(d, J = 8.0 Hz, 1H), 8.24-8.27(q, 1H); ^{13}C NMR (100 MHz,CDCl$_3$) δ 153.9, 141.9, 141.6, 137.4, 137.3, 134.6, 134.2, 134.0, 133.0, 131.5, 129.0, 128.7, 128.6, 128.4, 121.5, 117.9; ^{31}P NMR(200 MHz,CDCl$_3$) δ -4.26;

MS (ESI) m/z 582.0 [M]$^-$. HRMS (EI) m/z calcd for $C_{35}H_{22}O_4NPS$: 583.1002; Found 583.0988.

NP-2 was obtained as a yellow solid (40.7 mg, 0.07 mmol, 72%), ^{1}H NMR (400 MHz, CDCl$_3$) δ 2.10 (s, 1H), 6.45 (s, 1H), 6.91 (d, J = 8.0Hz, 1H), 7.02-7.05 (m, 1H), 7.30-7.37 (m, 10H), 7.48-7.54 (m, 2H), 7.63 (d, J = 12 Hz, 1H), 7.72-7.79 (m, 2H), 8.29 (d, J = 8.0 Hz, 1H), 8.33-8.36 (m, 1H), 8.69 (d, J = 8.0 Hz, 1H); ^{13}C NMR (100 MHz, CDCl$_3$) δ 183.9, 164.3, 151.0, 151.0, 146.4, 142.8, 134.2,134.0, 132.0, 128.9, 128.7, 128.6, 128.4, 127.5, 119.1, 118.9, 107.4, 8.7;δ^{31}P NMR(200 MHz,CDCl$_3$) δ -3.65; MS (ESI) m/z 604.0 [M+K]$^+$. HRMS (EI) m/z calcd for $C_{36}H_{24}O_4NP$: 565.1437; Found 565.1427.

NP-3 was obtained as a black solid (33.6 mg, 0.05 mmol, 50%), ^{1}H NMR (400 MHz, CDCl$_3$) δ1.79 (s, 6H),1.93(t, J = 6.0 Hz , 2H),2.71(t, J = 6.0 Hz , 2H), 2.83(t, J = 6.0 Hz , 2H), 4.17 (s, 3H), 6.80(dd, J = 8.4, 2.4 Hz, 1H), 6.86(d, J = 16 Hz , 1H),7.04(d, J = 8.0 Hz , 2H), 7.2 (s, 3H), 7.29-7.36 (m, 10H), 7.47-7.53 (m, 5H), 8.29-8.32 (m, 1H), 8.60 (d, J = 12 Hz, 1H), ^{13}C NMR (100 MHz, CDCl$_3$) 178.7, 159.6, 153.0, 152.4, 134.1, 133.9, 133.1, 129.4, 128.9, 128.7, 128.6, 128.5, 127.9, 122.1, 119.7, 119.1, 115.9,113.5, 109.6, 107.1, 106.5, 50.8, 34.1, 29.5, 28.0, 24.3, 20.2; ^{31}P NMR (200 MHz,CDCl$_3$) δ -4.27; MS (ESI) m/z 673.2 [M+H]$^+$. HRMS (EI) m/z calcd for $C_{45}H_{40}O_3NP$: 673.2740; Found 673.2773.

Cells culture and imaging using the probes NP-1~3

HeLa and A549 cells were incubated in MEM (modified Eagle's medium) supplemented with 10% FBS (fetal bovine serum) in an atmosphere of 5% CO$_2$ and 95% air at 37 °C, resepectively. The cells were plated in 35 mm glass-bottom culture dishes and allowed to adhere for 24 h. Before the experiments, the cells were washed with PBS buffer immediately. The cells were further incubated with probes **NP-1~3** for 20 min at 37 °C, After washing with PBS three times to remove the remaining probe, and then the cells were incubated in the absence or presence of AS in the culture medium for 45 min at 37 °C, and imaged with a Olympus FV1000 equipped with a CCD camera or Nikon A1R confocal microscope.

Fluorescence imaging in living mice using the probe NP-3

All animal procedures for this study were approved by the Animal Ethical Experimentation Committee of Shandong University according to the requirements of the National Act on the use of experimental animals (China). Kunming mice were anesthetized by an i.p. injection of xylazine (10 mg/kg) and ketamine (80 mg/kg). Then, the mice were intraperitoneally injected with probe **NP-3** (50 nanomoles). As a control, untreated mice (neither treated with AS nor probe **NP-3**) or mice intraperitoneally injected only with probe **NP-3** (50 nanomoles) were also prepared. The experiment group was given an i.p. injection of **NP-3** (50 nanomoles), and followed by i.p. injection with AS (500 nanomoles) after 30 min. The mice were then imaged (30 minutes after the injection of probe **NP-3**) using an IVIS Imaging System with excitation and emission filters set at 675 nm and Cy 5.5.

Results and Discussion

Design and synthesis of probes NP-1~3

Toward this end, we focused on the three structurally related
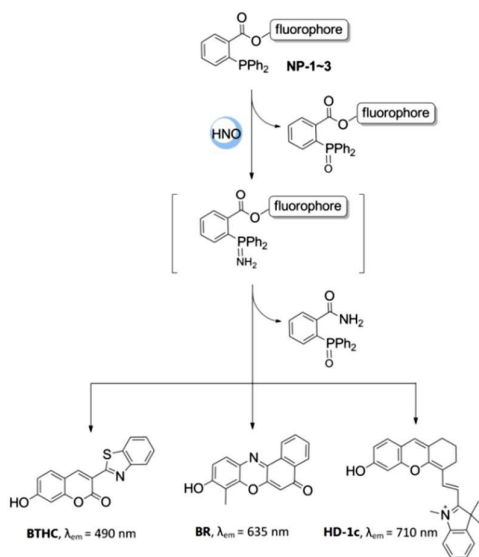
Scheme 1. Design strategy of the triarylphosphine-based fluorescent probes **NP-1~3** for multicolour imaging of HNO.

fluorophores, 3-benzothiazolyl-7-hydroxycoumarin (**BTHC**, λ_{em}= 490 nm),[41] benzoresorufin (**BR**, λ_{em}= 635 nm)[42] and our previously developed HD dye (**HD-1c**, λ_{em}= 710 nm).[12] These fluorophores have obviously different fluorescence colors in aqueous solution, as well as their emission spectra have relative small overlap and are well separated. In addition, they all possess hydroxyl which could serve as an optically tuneable group to control fluorescence. So, the three fluorophores were selected as the fluorescent platforms to construct novel probes for HNO. At the same time, we employed triphenylphosphine as the response site for HNO, because it has

selectively reactivity with HNO. With these considerations in mind, we developed three fluorescent probes (**NP-1~3**, Scheme 1), and speculated that the probes could show respond to HNO over a range of emission wavelengths from green to NIR and be useful for multicolor imaging of HNO in living system. To test the above-mentioned speculation, the probes (**NP-1~3**) were synthesized following the synthetic routes shown in Scheme S1 and fully characterized by ^{1}H NMR, ^{13}C NMR, ^{31}P NMR, MS (ESI), and HRMS (EI).

Sensing response of probes to HNO in PBS

With these probes in hand, we then investigated their optical properties in the absence or presence of HNO (Angeli's salt (AS) a commonly employed HNO donor). After reacting with AS in PBS, **NP-1~3** exhibited obvious new absorption bands located at 454 nm, 581nm and 695 nm, which can be attributed to the absorption of the dyes **BTHC**, **BR** and **HD-1c**, respectively (Fig. S1). As expected, due to the esterification of the hydroxyl groups, these probes exhibited very weak fluorescence with low fluorescence quantum yields (Φ < 0.015, shown in Table S1), which could cause low fluorescence background and be very critical for the highly sensitive detection of HNO. Upon treatment with AS, the fluorescence intensity at around 490 nm of **NP-1** increased dramatically in PBS buffer (pH 7.4, 25 mM, 10% ethanol) (Fig. 1A), and up to a 23-fold enhancement in fluorescence intensity was observed when the concentration of AS reached 14 equiv. Subsequently, we examined the fluorescence response of the other probes to HNO. As shown in Fig. 1B and 1C, the probes **NP-2** and **NP-3** both exhibited a fluorescence turn-on signal toward HNO, and the fluorescence signals could increase 8.5- and 11-fold for **NP-2** and **NP-3**, respectively. The detection limits for **NP-1~3** were calculated to be 6.48×10^{-7} M, 6.08×10^{-7} M and 6.22×10^{-7} M, respectively (Fig. S2), indicating that the probes are highly sensitive to HNO. To get insight into the probable response mechanism, we further decided to
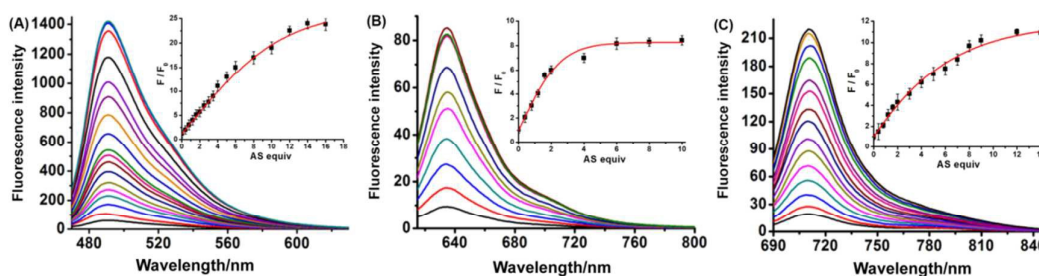
Fig. 1 (A) Fluorescence spectra of **NP-1** (5.0 µM) in pH 7.4 PBS buffer (10% ethanol) in the absence or presence of AS (0-90 µM). Inset: fluorescence intensity ratio (F / F$_0$) changes at 490 nm of NP-1 (5.0 µM) with the amount of AS. The spectra were recorded after incubation of the probe with AS for 45 min; (B) Fluorescence spectra of **NP-2** (10 µM) in pH 7.4 PBS buffer (30% ethanol) in the absence or presence of AS (0-100 µM). Inset: fluorescence intensity ratio (F / F$_0$) changes at 635 nm of **NP-2** (10 µM) with the amount of AS. The spectra were recorded after incubation of the probe with AS for 40 min; (C) Fluorescence spectra of **NP-3** (5.0 µM) in pH 7.4 PBS buffer (30% ethanol) in the absence or presence of AS (0-70 µM). Inset: fluorescence intensity ratio (F / F$_0$) changes at 710 nm of **NP-3** (5.0 µM) with the amount of AS. The spectra were recorded after incubation of the probe with AS for 45 min.
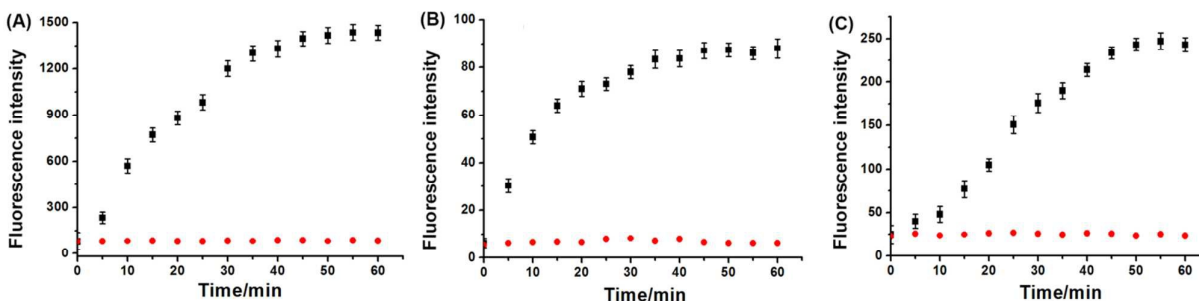
Fig. 2 Reaction-time profiles of **NP-1~3** in the absence [●] or presence of AS [■]. (A) The fluorescence intensities at 490 nm were continuously monitored at time intervals in pH 7.4 PBS buffer (10% ethanol). (B) The fluorescence intensities at 635 nm were continuously monitored at time intervals in pH 7.4 PBS buffer (30% ethanol). (C) The fluorescence intensities at 710 nm were continuously monitored at time intervals in pH 7.4 PBS buffer (30% ethanol). Time points represent 0, 5, 10, 15, 20, 25, 30, 35, 40, 45, 50, 55, and 60 min.
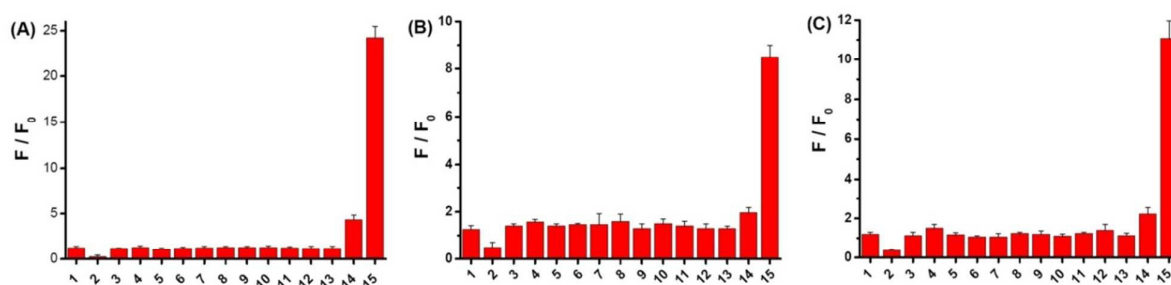
Fig. 3 The fluorescent responses of the probes **NP-1~3** to various relevant species (100 μM): 1. Blank; 2. ClO⁻; 3. H_2O_2; 4. sodium ascorbate; 5. $O_2^{•-}$; 6. NO; 7. NO_2^-; 8. NO_3^-, 9. N_3^-; 10. Fe^{3+}; 11. H_2S; 12. Cys; 13. GSH (1 mM); 14. GSNO; 15. AS. (A) **NP-1** (5 μM, in pH 7.4 PBS buffer containing 10% ethanol.); (B) **NP-2** (10 μM, in pH 7.4 PBS buffer containing 30% ethanol.); (C) **NP-3** (5.0 μM, in pH 7.4 PBS buffer containing 30% ethanol).

determine the products of **NP-1** (**NP-2**, **NP-3**) + AS by mass spectrometry (Fig. S3-5), and the results were consistent with the previous report that HNO could react with triarylphosphines to afford the corresponding phosphine oxide.[31-32]

Next, the time-dependent fluorescence spectra of **NP-1~3** in the absence or presence of HNO in PBS (pH = 7.4) were determined to study their reactivity toward HNO. As shown in Fig. 2, the marked increasements in the fluorescence intensities of **NP-1~3** were observed within a few minutes, and the emission intensities plateaued in about 45 minutes. These results suggest that the rapid fluorescence response of the probes may render it possible for the real-time detection of HNO. Furthermore, the probes **NP-1~3** could show obvious respond to HNO in the pH range from 7.0 to 8.5 (Fig. S6), indicating that the probes could exhibit fluorescent sensing response for HNO at physiological pH and may have potential usefulness in living system.

To examine the selectivity, the probes **NP-1~3** were incubated with various relevant analytes including reactive oxygen species (ROS), anions, small-molecule thiols, reducing agents, NO and HNO. As shown in Fig. 3, the representative species (ClO⁻, H_2O_2, Fe^{3+}, $O_2^{•-}$, sodium ascorbate, N_3^-, NO_2^-, NO_3^-, Cys, S^{2-}, NO at 100 μM, and GSH at 1 mM) elicited nearly no fluorescence response over 45 min. By contrast, only AS could cause significant enhancement in fluorescence intensity for the probes (23-fold, 8.5-fold and 11-fold

for **NP-1~3**, respectively). Furthermore, the introduction of 100 μM s-nitrosoglutathione (GSNO) to the probes induced only a small fluorescence enhancement and had nearly no interference to HNO detection. These data indicate that the probes show highly selective for HNO over the other relevant species.

In order to determine their usefulness as imaging reagents, the cytotoxicity of the probes toward A549 lung carcinoma cells and HeLa cells was further investigated. The living cells were incubated with various concentrations (5-30 μM) of **NP-1~3** for 24 h, and then the cell viability was determined by the standard 3-(4,5-dimethylthiazol-2-yl)-2,5-diphenyltetrazolium bromide (MTT) assays. The results indicate that the probes **NP-1~3** display no marked cytotoxicity at concentrations below 30 μM (Fig. S7-8). Thus, taken together, the probes **NP-1~3** could be potentially applied for detecting HNO in living system because of their prominent features including excellent selectivity, high sensitivity, favourable performance at physiological pH, relatively fast response, and low cytotoxicity.

Multicolour imaging of HNO in living cells

Encouraged by the above-mentioned desirable properties of the probes **NP-1~3**, we evaluated their capabilities to detect HNO in HeLa and A549 cells. As shown in Fig. 4, the HeLa cells incubated with only the probes **NP-1~3** at 37˚C for 20 min exhibited very weak
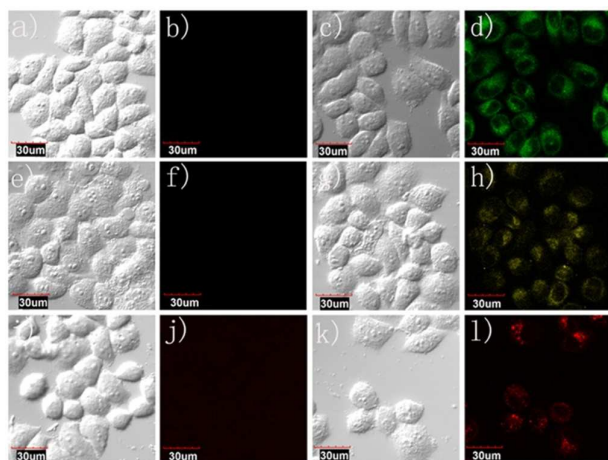
Fig. 4 Confocal fluorescence images of living HeLa cells using Olympus fluorescence microscopy: (a) Bright-field image of live HeLa cells incubated with only **NP-1** (5.0μM) for 20 min; (b) Fluorescence image of (a); (c) Bright-field image of live HeLa cells incubated with **NP-1** (5.0 μM) for 20 min, then with AS (75 μM) for 45 min; (d) Fluorescence image of (c). Excitation at 405 nm, emission window of 470-570 nm; (e) Bright-field image of live HeLa cells incubated with only **NP-2** (10 μM) for 20 min; (f) Fluorescence image of (e); (g) Bright-field image of live HeLa cells incubated with **NP-2** (10 μM) for 20 min, then with AS (100 μM) for 45 min; (h) Fluorescence image of (g). Excitation at 559 nm, emission window of 600-680 nm. (i) Bright-field image of live HeLa cells incubated with only **NP-3** (5.0 μM) for 20 min, (j) Fluorescence image of (i); (k) Bright-field image of live HeLa cells incubated with **NP-3** (5.0 μM) for 20 min, then with AS (75 μM) for 45 min; (k) Fluorescence image of (l). Excitation at 635 nm, emission window of 690-780 nm. Scale bar = 30 μm.
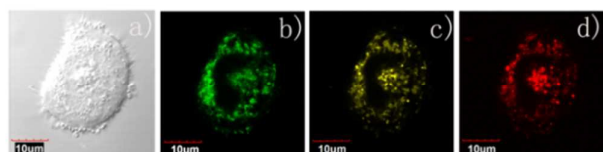
Fig. 5 Confocal fluorescence images of living HeLa cells using Olympus fluorescence microscopy: (a) Bright-field image of live HeLa cells incubated with **NP-1** (5.0 μM), **NP-2** (10 μM) and **NP-3** (5.0 μM) for 20 min, then with AS (200 μM) for 45 min; (b) Fluorescence image of (a), excitation at 405 nm, emission window of 470-570 nm; (c) Fluorescence image of (a), excitation at 559 nm, emission window of 600-680 nm; (d) Fluorescence image of (a), excitation at 635 nm, emission window of 690-780 nm. Scale bar = 10 μm.

fluorescence (Fig. 4b, 4f and 4j). By sharp contrast, when incubated with 5.0 μM probe **NP-1** for 20 min and then treated with 75 μM AS for another 45 min, HeLa cells could display strong fluorescence at the emission window of 470-570 nm (Fig. 4d). The HeLa cells also could show obviously enhanced fluorescence when they were incubated **NP-2** or **NP-3** for 20 min and then treated with 75 μM AS for another 45 min. Notably, the fluorescence colors of the probes **NP-1~3** in response to HNO in cells were changed from green to red, and were visually different. Similarly, the obvious turn-on fluorescence were observed when the A549 cells were incubated with probes **NP-1~3** respectively for 20 min and then treated with AS for another 45 min (Fig. S9). These data

indicate that the probes **NP-1~3** are probably suitable for multicolor imaging of HNO in living cells.

Subsequently, the multicolor imaging of HNO was investigated by incubating the same HeLa cells with the probes **NP-1~3** simultaneously in the presence of HNO. As shown in Fig. 5, when incubated with **NP-1** (5 μM), **NP-2** (10 μM) and **NP-3** (5 μM) for 20 min, and then treated with 200 μM AS for another 45 min, the HeLa cells showed distinct emission colors (from green to NIR) at different excitation wavelengths (Fig. 5b, c and d). Meanwhile, when incubated with **NP-1~3** simultaneously for 20 min and then treated with 200 μM AS for another 45 min, the A549 cells also can show distinct emission colors from green to NIR at different excitation wavelengths (Fig. S10). These data demonstrate that the probes **NP-1~3** could be successfully applied for multicolor imaging of HNO in living cells. This is the first report of the direct multicolor imaging of HNO with different emission wavelengths in living cells.

NIR imaging of HNO in living mice

Compared with the visible light (400-650 nm), the near-infrared (NIR) light (650-900 nm) is more suitable for the biological imaging in animal systems, because of its minimum photodamage and deep tissue penetration. When responding to HNO, **NP-3** can exhibit NIR fluorescence, while **NP-1** and **NP-2** showed fluorescence in the visible region. Therefore, we employed **NP-3** to determine its application for biological imaging in living mice using an IVIS imaging system with excitation and emission filters set at 675 nm and Cy 5.5, respectively. As shown in Fig. 6, when the mice were injected with the probe **NP-3** (50 nanomoles) in the peritoneal cavity, weak fluorescence was observed (Fig. 6b). However, the mice injected with the probe **NP-3** (50 nanomoles) and then treated by an i.p. injection with AS (500 nanomoles) exhibited
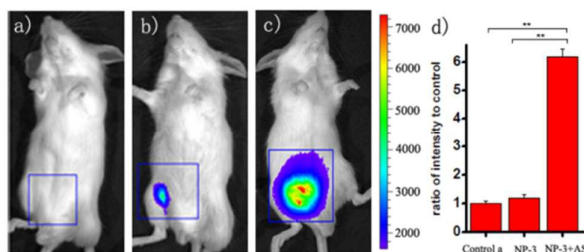
Fig. 6 Representative fluorescent images (*pseudo*color) of the mice: a) negative control, neither AS nor probe **NP-3** was injected; b) saline was injected in the intraperitoneal (i.p.) cavity of mice, followed by an i.p. injection of probe **NP-3** (50 nanomoles in DMSO); c) probe **NP-3** (50 nanomoles in DMSO) was injected into the peritoneal cavity of the mice, followed by an i.p. injection of AS (500 nanomoles in pH 7.4 PBS buffer). d) Quantification of fluorescence emission intensity from the groups a-c. The total number of photons from the entire peritoneal cavity of the groups a-c was integrated and plotted as a ratio to the control group a. Statistical analyses were performed with Student's *t*-test (n = 5). **P < 0.001 and error bars are ± s.d.
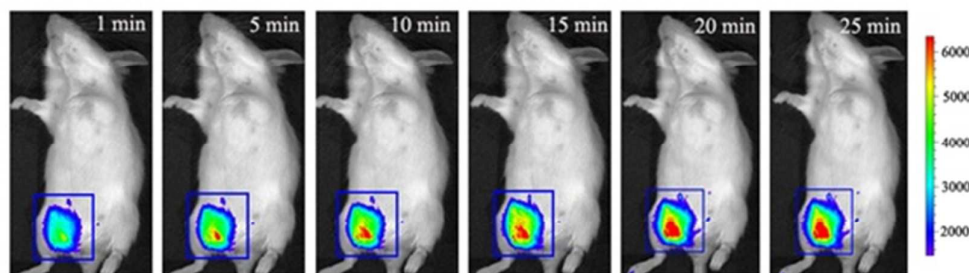
Fig. 7 Representative fluorescence images (*pseudo* color) of a Kunming mouse given an intraperitoneal (i.p.) injection of **NP-3** (50 nanomolesin DMSO) and a subsequent an intraperitoneal (i.p.) injection of AS (500 nanomolesin pH 7.4 PBS buffer). Images were taken after the incubation for 1, 5, 10, 15, 20, and 25 min, respectively.

significantly higher fluorescence readout (*pseudo*color) than the mice untreated (Fig. 6a) or treated with only the probe **NP-3** (Fig. 6b). Meanwhile, the quantified data of the fluorescence intensity from the abdominal area of the mice indicated that the mouse loaded with AS and the probe **NP-3** had an approximately 6-fold enhancement in the fluorescence intensity than the mice loaded with saline and the probe **NP-3** (Fig. 6d). Furthermore, the time-dependent (1, 5, 10, 15, 20, and 25 min) imaging of HNO in living mice was also conducted (Fig. 7). When injected with the probe **NP-3** (50 nanomoles) into the intraperitoneal cavity of the mice and followed treated by an i.p. injection of AS (500 nanomoles), a drastic enhancement in the fluorescence intensity was observed within 5 minutes, and the fluorescence intensity reached a maximum in 20 minutes approximately. Taken together, these results demonstrate that the new NIR probe **NP-3** is capable of sensing HNO in the living animals.

Conclusions

We have designed and synthesized three novel fluorescent turn-on probes **NP-1~3** for detecting HNO in living system. The probes **NP-1~3** exhibited desirable properties including high sensitivity, excellent selectivity, favourable performance at physiological pH, relatively fast response and low cytotoxicity to living cells. The probes could be separately applied for bioimaging of HNO in HeLa cells with different excitation and emission wavelengths. Importantly, when incubated with these probes simultaneously, the living cells could exhibit multicolor from green to near-infrared in the presence of HNO. The multicolor imaging of HNO with the help of multiple probes simultaneously, reported herein, could be beneficial for detecting HNO precisely in living system. Furthermore, the NIR fluorescent probe **NP-3** was suitable for fluorescence imaging of HNO not only in living cells, but also in living animals. The further applications of these fluorescent probes for the investigation of the biological functions and pathological roles of HNO in living systems are under progress. We also expect that the multicolour imaging method could be further applied for detecting other biomolecules including ROS and RNS precisely in living system.

Acknowledgements

Notes and references

1   J. M. Fukuto, C. J. Cisneros and R. L. Kinkade, *J Inorg. Biochem.,* **2013**, *118*, 201-208.

2   G. M.Johnson, T. J. Chozinski, E. S. Gallagher, C. A. Aspinwall and K. M. Miranda. *Free Radic. Biol. Med.,* **2014**, *76*, 299-307.

3   H. Nakagawa. *Nitric Oxide,* **2011**, *25*, 195-200.

4   S. E. Bari, M. A. Martí, V. T. Amorebieta, D. A. Estrin and F. Doctorovich.*J. Am. Chem. Soc.,* **2003**, *125*, 15272-15273.

5   Martí M. A.; Bari S. E.; D. A. Estrin and F. Doctorovich. *J. Am. Chem. Soc.,* **2005**, *127*, 4680-4684.

6   U. Samuni, Y. Samuni and S. Goldstein. *J. Am. Chem. Soc.,* **2010**, *132*, 8428-8432.

7   M. R. Cline, C. Tu, D. N. Silverman and J. P. Toscano.*Free Radic. Biol. Med.,* **2011**, *50*, 1274-1279.

8   S. A. Suárez, D. E. Bikiel, D. E. Wetzler, M. A. Martí and F. Doctorovich. *Anal. Chem.,* **2013**, *85*, 10262-10269.

9   X. Li, X. Gao, W. Shi and H. Ma.*Chem. Rev.,* **2014**, *114*, 590-659.

10   H. S. Jung, X. Chen, J. S. Kim and J. Yoon.*Chem. Soc. Rev.,* **2013**, *42*, 6019-6031.

11   Y.-J. Huang, W.-J. Ouyang, X. Wu, Z.Li, J. S. Fossey, T. D. James and Y.-B. Jiang. *J. Am. Chem. Soc.,* **2013**, *135*, 1700-1703.

12   L. Yuan, W. Lin, S. Zhao, W. Gao, B. Chen, L. He and S. Zhu. *J. Am. Chem. Soc.,* **2012**, *134*, 13510-13523.

13   C. Huang, T. Jia, M. Tang, Q. Yin, W. Zhu, C. Zhang, Y. Yang, N. Jia, Y. Xu and X. Qian. *J. Am. Chem. Soc.,* **2014**, *136*,14237-14244.

14   M.-Y. Wu, K. Li, Y.-H. Liu, K.-K. Yu, Y.-M. Xie, X.-D. Zhou and X.-Q. Yu. *Biomaterials,* **2015**, *53*, 669-678.

15   J. Tong, Y. Wang, J. Mei, J. Wang, A. Qin, J. Z. Sun and B. Z. Tang. *Chem. Eur. J.,* **2014**, *20*, 4661-4670.

16   X.-F. Yang, Q. Huang, Y. Zhong, Z. Li, H. Li, M. Lowry, J.O. Escobedo and R. M. Strongin. *Chem. Sci.,* **2014**, *5*, 2177-2183.

17   Matthew D. Hammers and Michael D. Pluth.Y.-W. Wang, S.-B. Liu, Y.-L. Yang, P.-Z. Wang, A.-J. Zhang and Y. Peng. *ACS Appl. Mater. Interfaces,* **2015**, *7*, 4415–4422.

18   W. Xuan, Y. Cao, J. Zhou and W. Wang. *Chem. Commun.,* **2013**, *49*, 10474-10476.

19   G. Song, Y. Sun, Y. Liu, X. Wang, M. Chen, F. Miao, W. Zhang, X. Yu and J. Jin. *Biomaterials,* **2014**, *35*, 2103-2112.

20   X. Zhang, C. Wang, Z. Han and Y. Xiao. *ACS Appl. Mater. Interfaces,* **2014**, *6*, 21669–21676.

21   W. Zhang, P. Li, F. Yang, X. Hu, C. Sun, W. Zhang, D. Chen and B. Tang *J. Am. Chem. Soc.,* **2013**, *135*, 14956-14959.

22   X. Wu, M. Yu, B. Lin, H. Xing, J. Han and S. Han. *Chem. Sci.,* **2015**, *6*, 798-803.

23   X.-L. Liu, X.-J. Du, C.-G. Dai and Q.-H. Song. *J. Org. Chem.,* **2014**, *79*, 9481-9489.

24   X. Shen, G. Zhang and D. Zhang. *Org. Lett.,* **2012**, *14*,1744-1747.

25   Q. Wan, S. Chen, W. Shi, L. Li and H. Ma. *Angew. Chem. Int. Ed.,* **2014**, *53*, 10916-10920.

26   A. T. Wrobel, T. C. Johnstone, A. D. Liang, S. J. Lippard and P. Rivera-Fuentes. *J. Am. Chem. Soc.* **2014**, *136*, 4697-4705.

27   Y. Zhou, K. Liu, J.-Y. Li, Y. Fang, T.-C. Zhao and C. Yao. *Org. Lett.,* **2011**, *13*, 1290-1293.

28   C. Liu,H. Wu,Z. Wang,C. Shao,B. Zhu andX. Zhang, *Chem. Commun.*, **2014**, *50*, 6013-6016.

29   P. Liu,X. Jing,F. Yu, C.Lvand L. Chen, *Analyst*, **2015**, *140*, 4576-4583.

30   X. Jing,F. Yu and L. Chen, *Chem. Commun.*, **2014**,*50*, 14253-14256.

31   C. Liu, H. Wu, Z. Wang, C.Shao, B. Zhu and X. Zhang. *Chem. Commun.,* **2014**, *50*, 6013-6016.

32   K. Kawai, N. Ieda, K. Aizawa, T. Suzuki, N. Miyata and H. Nakagawa. *J. Am. Chem. Soc.* **2013**, 135, 12690-12696.

33   X. Jing, F. Yu, L. Chen. *Chem. Commun.,* **2014**, *50*, 14253-14256.

34   K. Zheng, W. Lin, D. Cheng, H. Chen, Y. Liu and K. Liu.*Chem. Commun.,* **2015**, *51*, 5754-5757.

35   H. Zhang, R. Liu, Y. Tan, W. H. Xie, H. Lei, H.-Y. Cheung and H. Sun. *ACS Appl. Mater. Interfaces,* **2015**, *7*, 5438-5443.

36   G.-J. Mao, X.-B. Zhang, X. -L. Shi, H-W. Liu, Y.-X. Wu, L.-Y. Zhou, W. Tan and R.-Q. Yu, *Chem. Commun.,* **2014**,50, 5790-5792.

37   B. C. Dickinson, C. Huynh and C. J. Chang. *J. Am. Chem. Soc.* **2010**, *132*, 5906-5915.

38   B. N.Giepmans, S. R.Adams, M. H.Ellisman and R. Y.Tsien. *Science* **2006**, 312, 217-224.

39   N. C. Shaner, P. A. Steinbach and R. Y. Tsien. *Nat. Methods,* **2005**, *2*, 905-909.

40   S. T Laughlin and C. R.Bertozzi. *Proc. Natl. Acad. Sci. U.S.A.,* **2009**, *106*,12-17.

41   W. Lin, L. Long and W. Tan. *Chem. Commun.,* **2010**, *46*, 1503-1505.

42   U.-P. Apfel, D. Buccella, J. J. Wilson and S.J. Lippard. *Inorg. Chem.,* **2013**, *52*, 3285-3294.